Results in Physics 33 (2022) 105128

Contents lists available at ScienceDirect

Results in Physics

journal homepage: www.elsevier.com/locate/rinp

Doubly periodic wave structure of the modified Schrödinger equation with fractional temporal evolution

Pinki Kumari [a], R.K. Gupta [a,b], Sachin Kumar [a,*], K.S. Nisar [c]

[a] Department of Mathematics and Statistics, School of Basic Sciences, Central University of Punjab, Bathinda, Punjab, India
[b] Department of Mathematics, School of Basic Sciences, Central University of Haryana, Mahendergarh, Haryana, India
[c] Department of Mathematics, College of Arts and Sciences, Prince Sattam bin Abdulaziz University, Wadi Aldawaser, 11991, Saudi Arabia

ARTICLE INFO

Keywords:
Schrödinger equation
Generalized Jacobi elliptic function
Conformable operator

ABSTRACT

Abundant Jacobi elliptic type solutions with distinct physical structures of complex nonlinear conformable time-fractional modified Schrödinger equation are obtained by using the generalized Jacobi elliptic function (GJEF) method. The Jacobi function expansions may lead to new doubly periodic wave solutions, soliton solutions, and triangular periodic solutions. Nowadays the conformable operator is being used for a better description of the dynamical systems. Motivated by the potential applications of the governed equation in nonlinear optics, biological sciences, and fluid dynamics, these solutions may be significant in the study of wave propagation in the desired field. Symbolic computations are made with the aid of Maple.

Introduction

In recent times, the theory of nonlinear equations has seen remarkable developments. The partial differential equations are the mathematical formulations of the laws of nature. Various fields of engineering, applied sciences and mathematical physics use them in the mathematical analysis of diverse physical phenomena [1]. The exact solution of a differential equation is very helpful in interpreting it with its physical and mathematical applications. Many methods have been developed to find various kinds of solutions like lump, kink, breather-type, invariant, periodic cross-kink type etc., of nonlinear partial differential systems [2–17]. In recent studies, many techniques have been developed to find waveform, solitonic type, periodic or explicit solutions of conformable fractional differential (CFD) equations [6,18–23].

Governing equation

We consider the complex nonlinear conformable time fractional modified Schrödinger equation [24,25], which is expressed as

$$\imath w_t^{\alpha} + w_{xx} + |w|^2 w + \imath\varepsilon (w_{xxx} + k_1 |w|^2 w_x + k_2 w^2 w_x^*) = 0, \tag{1}$$

where $w(x,t)$ is an unknown complex function, w^* is the complex conjugate of w, $\alpha \in (0,1)$ and subscripts denote partial derivatives with respect to x and t; k_1, k_2, ε are constants, $\imath^2 = -1$ and w_t^{α} is the conformable fractional derivative [26].

The Eq. (1) can be reduced to a nonlinear integrable cubic Schrödinger equation when $\varepsilon = 0$ and $\alpha = 1$. The optical soliton solutions of nonlinear conformable fractional cubic Schrödinger equation are reported in Ref. [27]. When $k_1 = 3k_2$, it becomes the Sasa–Satsuma equation [10] while for $k_2 = 0$, the equation is referred to as Hirota equation [24]. The exact solutions of (1) are presented by Lie classical method [28].

The applications of (1) appear in nonlinear optics and biological phenomena. In the context of biological science, Eq. (1) is known as generalized Davydov equation [29] which arises in the study of nonlinear dynamics of α- helical protein in DNA molecules.

In the context of nonlinear optics, with the switching of independent variables $t \leftrightarrow x$, (1) describes the propagation of femtosecond pulses in a monomode optical fiber as a model of a long-distance-high-bit-rate transmission system. In this interpretation, w characterizes the slowly-varying envelope of the electromagnetic field. The coefficients ε, k_1, k_2 occur from the perturbation effects and denote the group velocity dispersion, self-phase modulation, dispersion, self steepening, and self-frequency shift by virtue of stimulated Raman scattering respectively.

The concept of conformable fractional derivative (CFD) is introduced by Khalil et al. [30], which is defined as

Definition 0.1. Given a function $f : [0,\infty) \to R$. Then the "conformable fractional derivative" of order α is defined by

$$T_{\alpha}(f)(t) = \lim_{\epsilon \to 0} \frac{f(t + \epsilon t^{1-\alpha}) - f(t)}{\epsilon} \tag{2}$$

* Corresponding author.
E-mail addresses: yadav.pk1403@gmail.com (P. Kumari), rajeshgupta@cuh.ac.in (R.K. Gupta), sachin1jan@yahoo.com (S. Kumar), n.sooppy@psau.edu.sa (K.S. Nisar).

https://doi.org/10.1016/j.rinp.2021.105128
Received 13 November 2021; Received in revised form 11 December 2021; Accepted 12 December 2021
Available online 1 January 2022

for all $t > 0, \alpha \in (0,1)$. If f is α-differentiable in some $(0,a), a > 0$, and $\lim_{t\to 0^+} f^{\alpha}(t)$ exists, then define $f^{\alpha}(0) = \lim_{t\to 0^+} f^{\alpha}(t)$.

The physical and geometrical interpretations of CFD thus indicate potential applications in physics and engineering [31]. The major advantage of this natural definition is that this overcomes the inconsistencies that occurred on comparing the existing fractional derivative definitions with Newton's derivative. The compatibility of this definition with the classical derivative makes the results of the nonlinear fractional equation helpful for both fractional as well integer order partial differential equations (PDEs) by taking α integer or fraction in a single study. So with this advantage, there is much scope in this direction.

In this study, we implement GJEF method [32,33] to acquire new solitary and wave solutions of (1). Basically, the method uses the advantage of the solutions of the auxiliary ordinary differential equation to construct a rich variety of Jacobian elliptic solutions. To the best of my information, the technique is used for the first time in the context of conformable fractional partial differential equations.

Outline of generalized Jacobi elliptic function method

In this section, the main steps of the generalized Jacobi elliptic function expansion method for the conformable fractional equation are briefly described.

Step1: Consider a general time conformable fractional evolution equation as follows:

$$F(u, \frac{\partial^{\alpha} u}{\partial t^{\alpha}}, \frac{\partial u}{\partial x}, \frac{\partial^{2\alpha} u}{\partial t^{2\alpha}}, \frac{\partial u}{\partial x}, \ldots) = 0. \tag{3}$$

By employing the wave transformation

$$u(x,t) = U(\xi), \quad \xi = kx - v\frac{t^{\alpha}}{\alpha}, \tag{4}$$

and using the chain rule [26], (3) reduces into an ordinary differential equation (ODE),

$$L(U, U', U'', \ldots) = 0, \tag{5}$$

where $'$ denotes first order derivative w.r.t. ξ.

Step 2: Assume that the solution of (5) takes the following form:

$$U(\xi) = \sum_{i=-s}^{s} a_i F^i(\xi). \tag{6}$$

Here, the functions $F(\xi)$ are the solutions of the following ODE:

$$(F')^2(\xi) = PF^4(\xi) + QF^2(\xi) + R, \tag{7}$$

which are given in Table 1 for different values of constants P, Q and R.

Step3: By using the balancing principle, s can be determined. Then inserting (6) into (5), and equating the coefficients of polynomial in F to zero, a system of algebraic equations is yielded. On solving that system, we can determine a_i, k, v.

Step 4: By utilizing all values of P, Q, R and gathering all the results given in Table 1, the exact solutions of (3) can be obtained.

Note 1: The functions F, written in Table 1 are double periodic, Jacobi elliptic functions $cn = cn(\xi,m), sn = sn(\xi,m), dn = dn(\xi,m)$ and m $(0 < m < 1)$ is the modulus of elliptic functions.

Application to conformable modified Schrodinger equation

In this section, we will employ the GJEF method on the conformable time fractional modified Schrödinger equation (1). In what follows, we first consider the gauge transformation

$$w(x,t) = H(\xi)e^{\iota(ax - b\frac{t^{\alpha}}{\alpha} + c)}, \quad \xi = kx - v\frac{t^{\alpha}}{\alpha}, \tag{8}$$

Table 1
Solutions of (7) for some values of P, Q and R [34,35].

P	Q	R	F
m^2	$-(1+m^2)$	1	sn, cd
$-m^2$	$2m^2-1$	$1-m^2$	cn
-1	$2-m^2$	m^2-1	dn
1	$-(1+m^2)$	m^2	ns, dc
$1-m^2$	$2m^2-1$	$-m^2$	nc
m^2-1	$2-m^2$	-1	nd
$1-m^2$	$2-m^2$	1	sc
$-m^2(1-m^2)$	$2m^2-1$	1	sd
1	$2-m^2$	$1-m^2$	cs
1	$2m^2-1$	$-m^2(1-m^2)$	ds
$\frac{-1}{4}$	$\frac{m^2+1}{2}$	$\frac{-(1-m^2)^2}{4}$	$mcn \mp dn$
$\frac{1}{4}$	$\frac{1-2m^2}{2}$	$\frac{1}{4}$	$ns \mp cs$
$\frac{1-m^2}{4}$	$\frac{m^2+1}{2}$	$\frac{1-m^2}{4}$	$nc \mp sc$
$\frac{1}{4}$	$\frac{m^2-2}{2}$	$\frac{m^4}{4}$	$ns \mp ds$
$\frac{m^2}{4}$	$\frac{m^2-2}{2}$	$\frac{m^4}{4}$	$sn \mp \iota cn, \frac{dn}{\sqrt{1-m^2}sn \mp cn}$
$\frac{1}{4}$	$\frac{1-2m^2}{2}$	$\frac{1}{4}$	$mcn \mp \iota dn, \frac{sn}{1 \mp cn}$
$\frac{m^2}{4}$	$\frac{m^2-2}{2}$	$\frac{1}{4}$	$\frac{sn}{1 \mp dn}$
$\frac{m^2-1}{4}$	$\frac{m^2+1}{2}$	$\frac{m^2-1}{4}$	$\frac{dn}{1 \mp rsn}$
$\frac{1-m^2}{4}$	$\frac{m^2+1}{2}$	$\frac{1-m^2}{4}$	$\frac{cn}{1 \mp sn}$
$\frac{(1-m^2)^2}{4}$	$\frac{m^2+1}{2}$	$\frac{1}{4}$	$\frac{sn}{dn \mp cn}$
$\frac{m^4}{4}$	$\frac{m^2-1}{2}$	$\frac{1}{4}$	$\frac{cn}{\sqrt{1-m^2} \mp dn}$

which decomposes (1) into the following ODE:

$$k^3 \varepsilon H'' - (a^2 - b - a^3\varepsilon)H + \frac{(k_1 + k_2)}{3} k\varepsilon H^3 = 0, \tag{9}$$

by selecting

$$k_2 = \frac{3 - k_1}{2k\varepsilon - 1}, \; a = \frac{1 - k\varepsilon}{3\varepsilon}, \; v = a^2 - b - a^3\varepsilon + 2ak - 3a^2\varepsilon k. \tag{10}$$

Here $H, \frac{v}{k}, a, b,$ and c denotes the pulse shape, wave speed, wave frequency, wave number and phase constant respectively.

By using balancing principle, we get $s = 1$. So, the solution of (9) is assumed of the form

$$H(\xi) = \frac{a_{-1}}{F(\xi)} + a_0 + a_1 F(\xi). \tag{11}$$

By substituting (11) into (9), the following set of algebraic equations are obtained:

$$\begin{aligned}
&2\,k^3\epsilon\, P a_1 + \frac{1}{3}\left(k_1 + k_2\right) k\varepsilon\, a_1^3 = 0,\\
&\left(k_1 + k_2\right) k\varepsilon\, a_0 a_1^2 = 0,\\
&k^3\epsilon\, Q a_1 - \left(-a^3\epsilon + a^2 - b\right) a_1 + \frac{1}{3}\left(k_1 + k_2\right) k\varepsilon\, \left(a_{-1}{a_1}^2 + 2\,{a_0}^2 a_1\right.\\
&\left. +\, a_1\left(2\,a_{-1}a_1 + {a_0}^2\right)\right) = 0,\\
&\left(-a^3\epsilon + a^2 - b\right) a_0 + \frac{1}{3}\left(k_1 + k_2\right) k\varepsilon\, \left(4\,a_{-1}a_0 a_1 + a_0\left(2\,a_{-1}a_1 + {a_0}^2\right)\right) = 0,\\
&k^3\epsilon\, Q a_{-1} - \left(-a^3\epsilon + a^2 - b\right) a_{-1} + \frac{1}{3}\left(k_1 + k_2\right) k\varepsilon\, \left(a_{-1}\left(2\,a_{-1}a_1 + {a_0}^2\right)\right.\\
&\left. +\, 2\,{a_0}^2 a_{-1} + a_1{a_{-1}}^2\right) = 0,\\
&\left(k_1 + k_2\right) k\varepsilon\, {a_{-1}}^2 a_0 = 0,\\
&2\,k^3\epsilon\, R a_{-1} + \frac{1}{3}\left(k_1 + k_2\right) k\varepsilon\, {a_{-1}}^3 = 0.
\end{aligned} \tag{12}$$

On solving the above system with the aid of maple, we have

$$a_{-1} = \iota\sqrt{\frac{6R}{k_1 + k_2}}k, \; a_0 = 0, \; a_1 = \iota\sqrt{\frac{6P}{k_1 + k_2}}k, \quad b = a^2 - a^3\varepsilon - \varepsilon\left(Q - 6\sqrt{PR}\right)k^3. \tag{13}$$

Subsequently, by selecting the appropriate values of P, Q and R from Table 1 and collecting the values together with (11), we obtain the analytic solutions of (1) as follows.

(i) $P = m^2,\ Q = -(1+m^2),\ R = 1, \xi = kx - v\frac{t^\alpha}{\alpha},\ b = a^2 - a^3\varepsilon - \varepsilon\left(Q - 6\sqrt{PR}\right)k^3$.

$$w_1(x,t) = \left(\imath\sqrt{\frac{6}{k_1+k_2}}k\left(\frac{1}{sn(\xi)}\right) + \imath\sqrt{\frac{6m^2}{k_1+k_2}}ksn(\xi)\right)e^{\imath(ax - b\frac{t^\alpha}{\alpha}+c)}, \quad (14)$$

and

$$w_2(x,t) = \left(\imath\sqrt{\frac{6}{k_1+k_2}}k\left(\frac{1}{cd(\xi)}\right) + \imath\sqrt{\frac{6m^2}{k_1+k_2}}kcd(\xi)\right)e^{\imath(ax - b\frac{t^\alpha}{\alpha}+c)}. \quad (15)$$

(ii) $P = -m^2,\ Q = 2m^2 - 1,\ R = 1 - m^2, \xi = kx - v\frac{t^\alpha}{\alpha},\ b = a^2 - a^3\varepsilon - \varepsilon\left(Q - 6\sqrt{PR}\right)k^3$.

$$w_3(x,t) = \left(\imath\sqrt{\frac{6(1-m^2)}{k_1+k_2}}k\left(\frac{1}{cn(\xi)}\right) - \sqrt{\frac{6m^2}{k_1+k_2}}kcn(\xi)\right)e^{\imath(ax - b\frac{t^\alpha}{\alpha}+c)}. \quad (16)$$

(iii) $P = -1,\ Q = 2 - m^2,\ R = m^2 - 1, \xi = kx - v\frac{t^\alpha}{\alpha},\ b = a^2 - a^3\varepsilon - \varepsilon\left(Q - 6\sqrt{PR}\right)k^3$.

$$w_4(x,t) = \left(\imath\sqrt{\frac{6(m^2-1)}{k_1+k_2}}k\left(\frac{1}{dn(\xi)}\right) - \sqrt{\frac{6}{k_1+k_2}}kdn(\xi)\right)e^{\imath(ax - b\frac{t^\alpha}{\alpha}+c)}. \quad (17)$$

(iv) $P = 1,\ Q = -(1+m^2),\ R = m^2, \xi = kx - v\frac{t^\alpha}{\alpha},\ b = a^2 - a^3\varepsilon - \varepsilon\left(Q - 6\sqrt{PR}\right)k^3$.

$$w_5(x,t) = \left(\imath\sqrt{\frac{6m^2}{k_1+k_2}}k\left(\frac{1}{ns(\xi)}\right) + \imath\sqrt{\frac{6}{k_1+k_2}}kns(\xi)\right)e^{\imath(ax - b\frac{t^\alpha}{\alpha}+c)}, \quad (18)$$

$$w_6(x,t) = \left(\imath\sqrt{\frac{6m^2}{k_1+k_2}}k\left(\frac{1}{dc(\xi)}\right) + \imath\sqrt{\frac{6}{k_1+k_2}}kdc(\xi)\right)e^{\imath(ax - b\frac{t^\alpha}{\alpha}+c)}. \quad (19)$$

(v) $P = 1 - m^2,\ Q = 2m^2 - 1,\ R = -m^2, \xi = kx - v\frac{t^\alpha}{\alpha},\ b = a^2 - a^3\varepsilon - \varepsilon\left(Q - 6\sqrt{PR}\right)k^3$.

$$w_7(x,t) = \left(-\sqrt{\frac{6m^2}{k_1+k_2}}k\left(\frac{1}{nc(\xi)}\right) + \imath\sqrt{\frac{6(1-m^2)}{k_1+k_2}}knc(\xi)\right)e^{\imath(ax - b\frac{t^\alpha}{\alpha}+c)}. \quad (20)$$

(vi) $P = m^2 - 1,\ Q = 2 - m^2,\ R = -1, \xi = kx - v\frac{t^\alpha}{\alpha},\ b = a^2 - a^3\varepsilon - \varepsilon\left(Q - 6\sqrt{PR}\right)k^3$.

$$w_8(x,t) = \left(-\sqrt{\frac{6}{k_1+k_2}}k\left(\frac{1}{nd(\xi)}\right) + \imath\sqrt{\frac{6(m^2-1)}{k_1+k_2}}knd(\xi)\right)e^{\imath(ax - b\frac{t^\alpha}{\alpha}+c)}. \quad (21)$$

(vii) $P = 1 - m^2,\ Q = 2 - m^2,\ R = 1, \xi = kx - v\frac{t^\alpha}{\alpha},\ b = a^2 - a^3\varepsilon - \varepsilon\left(Q - 6\sqrt{PR}\right)k^3$.

$$w_9(x,t) = \left(\imath\sqrt{\frac{6}{k_1+k_2}}k\left(\frac{1}{sc(\xi)}\right) + \imath\sqrt{\frac{6(1-m^2)}{k_1+k_2}}ksc(\xi)\right)e^{\imath(ax - b\frac{t^\alpha}{\alpha}+c)}. \quad (22)$$

(viii) $P = -m^2(1-m^2),\ Q = 2m^2 - 1,\ R = 1, \xi = kx - v\frac{t^\alpha}{\alpha},\ b = a^2 - a^3\varepsilon - \varepsilon\left(Q - 6\sqrt{PR}\right)k^3$.

$$w_{10}(x,t) = \left(\imath\sqrt{\frac{6}{k_1+k_2}}k\left(\frac{1}{sd(\xi)}\right) - \sqrt{\frac{6m^2(1-m^2)}{k_1+k_2}}ksd(\xi)\right)e^{\imath(ax - b\frac{t^\alpha}{\alpha}+c)}. \quad (23)$$

(ix) $P = 1,\ Q = 2 - m^2,\ R = 1 - m^2, \xi = kx - v\frac{t^\alpha}{\alpha},\ b = a^2 - a^3\varepsilon - \varepsilon\left(Q - 6\sqrt{PR}\right)k^3$.

$$w_{11}(x,t) = \left(\imath\sqrt{\frac{6}{k_1+k_2}}k\left(\frac{1}{cs(\xi)}\right) + \imath\sqrt{\frac{6m^2}{k_1+k_2}}kcs(\xi)\right)e^{\imath(ax - b\frac{t^\alpha}{\alpha}+c)}. \quad (24)$$

(x) $P = 1,\ Q = 2m^2 - 1,\ R = -m^2(1-m^2), \xi = kx - v\frac{t^\alpha}{\alpha},\ b = a^2 - a^3\varepsilon - \varepsilon\left(Q - 6\sqrt{PR}\right)k^3$

$$w_{12}(x,t) = \left(-\sqrt{\frac{6m^2(1-m^2)}{k_1+k_2}}k\left(\frac{1}{ds(\xi)}\right) + \imath\sqrt{\frac{6}{k_1+k_2}}kds(\xi)\right)e^{\imath(ax - b\frac{t^\alpha}{\alpha}+c)}. \quad (25)$$

(xi) $P = -\frac{1}{4},\ Q = \frac{1+m^2}{2},\ R = -\frac{(1-m^2)^2}{4}, \xi = kx - v\frac{t^\alpha}{\alpha},\ b = a^2 - a^3\varepsilon - \varepsilon\left(Q - 6\sqrt{PR}\right)k^3$.

$$w_{13}(x,t) = \left(-\sqrt{\frac{6(1-m^2)^2}{4k_1+4k_2}}k\left(\frac{1}{mcn(\xi) \mp dn(\xi)}\right) - \sqrt{\frac{6}{4k_1+4k_2}}k(mcn(\xi) \mp dn(\xi))\right)e^{\imath(ax - b\frac{t^\alpha}{\alpha}+c)}. \quad (26)$$

(xii) $P = \frac{1}{4},\ Q = \frac{1-2m^2}{2},\ R = \frac{1}{4}, \xi = kx - v\frac{t^\alpha}{\alpha},\ b = a^2 - a^3\varepsilon - \varepsilon\left(Q - 6\sqrt{PR}\right)k^3$.

$$w_{14}(x,t) = \left(\imath\sqrt{\frac{6}{4k_1+4k_2}}k\left(\frac{1}{ns(\xi) \mp cs(\xi)}\right) + \imath\sqrt{\frac{6}{4k_1+4k_2}}k(ns(\xi) \mp cs(\xi))\right)e^{\imath(ax - b\frac{t^\alpha}{\alpha}+c)}. \quad (27)$$

(xiii) $P = \frac{1-m^2}{4},\ Q = \frac{1+m^2}{2},\ R = \frac{1-m^2}{4}, \xi = kx - v\frac{t^\alpha}{\alpha},\ b = a^2 - a^3\varepsilon - \varepsilon\left(Q - 6\sqrt{PR}\right)k^3$.

$$w_{15}(x,t) = \left(\imath\sqrt{\frac{6(1-m^2)}{4k_1+4k_2}}k\left(\frac{1}{nc(\xi) \mp sc(\xi)}\right) + \imath\sqrt{\frac{6(1-m^2)}{4k_1+4k_2}}k(nc(\xi) \mp sc(\xi))\right)e^{\imath(ax - b\frac{t^\alpha}{\alpha}+c)}. \quad (28)$$

(xiv) $P = \frac{1}{4},\ Q = \frac{m^2-2}{2},\ R = \frac{m^4}{4}, \xi = kx - v\frac{t^\alpha}{\alpha},\ b = a^2 - a^3\varepsilon - \varepsilon\left(Q - 6\sqrt{PR}\right)k^3$.

$$w_{16}(x,t) = \left(\imath\sqrt{\frac{6m^4}{4k_1+4k_2}}k\left(\frac{1}{ns(\xi) \mp ds(\xi)}\right) + \imath\sqrt{\frac{6}{4k_1+4k_2}}k(ns(\xi) \mp ds(\xi))\right)e^{\imath(ax - b\frac{t^\alpha}{\alpha}+c)}. \quad (29)$$

(xv) $P = \frac{m^2}{4},\ Q = \frac{m^2-2}{2},\ R = \frac{m^2}{4}, \xi = kx - v\frac{t^\alpha}{\alpha},\ b = a^2 - a^3\varepsilon - \varepsilon\left(Q - 6\sqrt{PR}\right)k^3$.

$$w_{17}(x,t) = \left(\imath\sqrt{\frac{6(1-m^2)}{4k_1+4k_2}}k\left(\frac{1}{sn(\xi) \mp \imath cn(\xi)}\right) + \imath\sqrt{\frac{6(1-m^2)}{4k_1+4k_2}}k(sn(\xi) \mp \imath cn(\xi))\right)e^{\imath(ax - b\frac{t^\alpha}{\alpha}+c)}. \quad (30)$$

$$w_{18}(x,t) = \imath\sqrt{\frac{6(1-m^2)}{4k_1+4k_2}}k\left(\frac{(\sqrt{1-m^2}sn(\xi) \mp cn(\xi))^2 + dn^2(\xi)}{dn(\xi)(\sqrt{1-m^2}sn(\xi) \mp cn(\xi))}\right)e^{\imath(ax - b\frac{t^\alpha}{\alpha}+c)}. \quad (31)$$

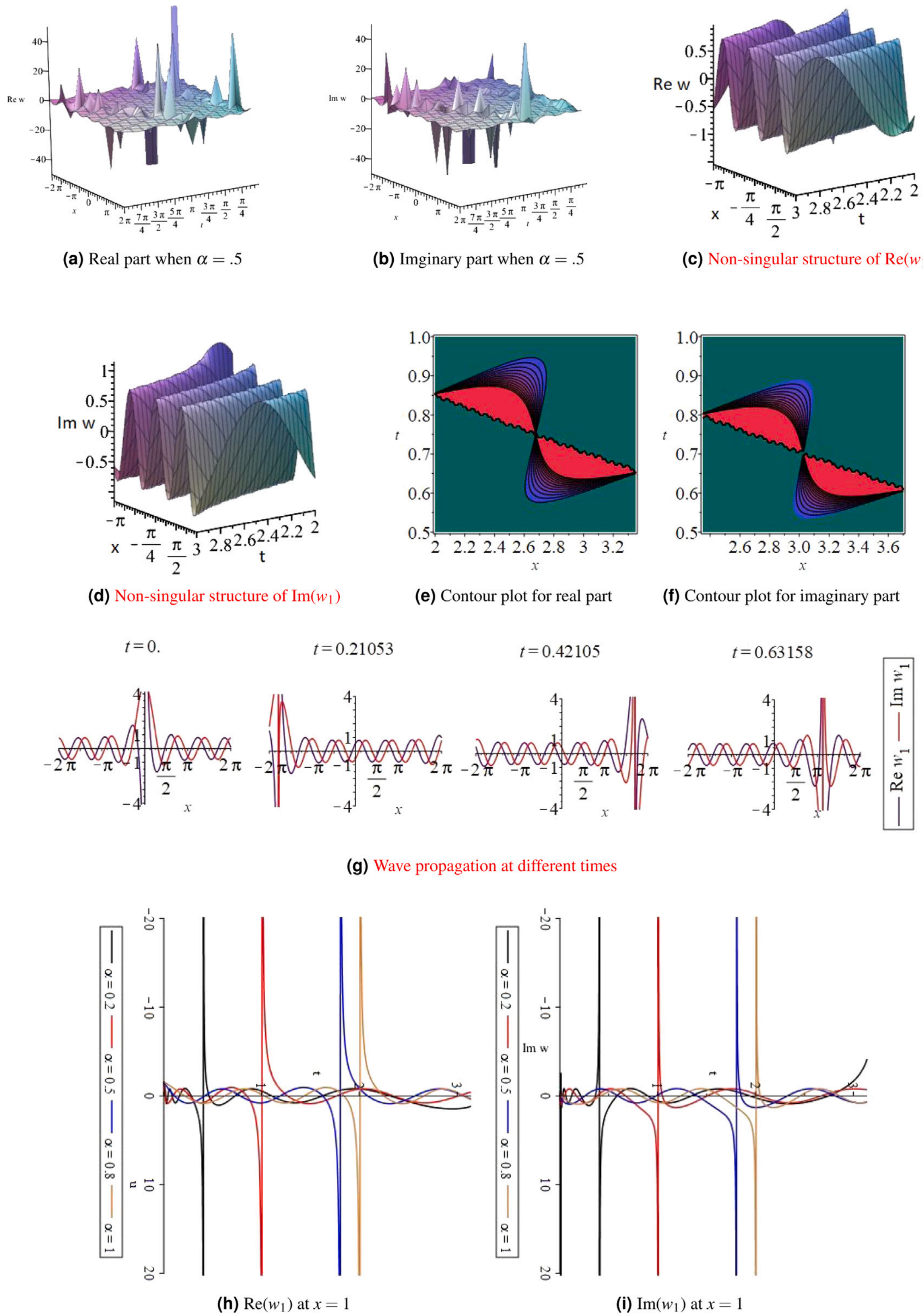

(a) Real part when $\alpha = .5$ **(b)** Imginary part when $\alpha = .5$ **(c)** Non-singular structure of Re(w_1)

(d) Non-singular structure of Im(w_1) **(e)** Contour plot for real part **(f)** Contour plot for imaginary part

(g) Wave propagation at different times

(h) Re(w_1) at $x = 1$ **(i)** Im(w_1) at $x = 1$

Fig. 1. Profiles of (14) with the parametric values $k_1 = 0.2, m = 0.8, \alpha = 0.5, k = 0.3, c = 0, \epsilon = 0.1$.

(xvi) $P = \frac{1}{4}$, $Q = \frac{1-2m^2}{2}$, $R = \frac{1}{4}, \xi = kx - v\frac{t^\alpha}{\alpha}$, $b = a^2 - a^3\epsilon - \epsilon\left(Q - 6\sqrt{PR}\right)k^3$.

$$w_{19}(x,t) = \Bigg(\imath\sqrt{\frac{6}{4k_1+4k_2}}k\Big(\frac{1}{mcn(\xi) \mp \imath dn(\xi)}\Big) + \imath\sqrt{\frac{6}{4k_1+4k_2}}k(mcn(\xi) \mp \imath dn(\xi)) \Bigg) e^{\imath(ax-b\frac{t^\alpha}{\alpha}+c)}. \tag{32}$$

$$w_{20}(x,t) = \Bigg(\imath\sqrt{\frac{6}{4k_1+4k_2}}k\Big(\frac{1 \mp cn(\xi)}{sn(\xi)}\Big) + \imath\sqrt{\frac{6}{4k_1+4k_2}}k\Big(\frac{sn(\xi)}{1 \mp cn(\xi)}\Big) \Bigg) e^{\imath(ax-b\frac{t^\alpha}{\alpha}+c)}. \tag{33}$$

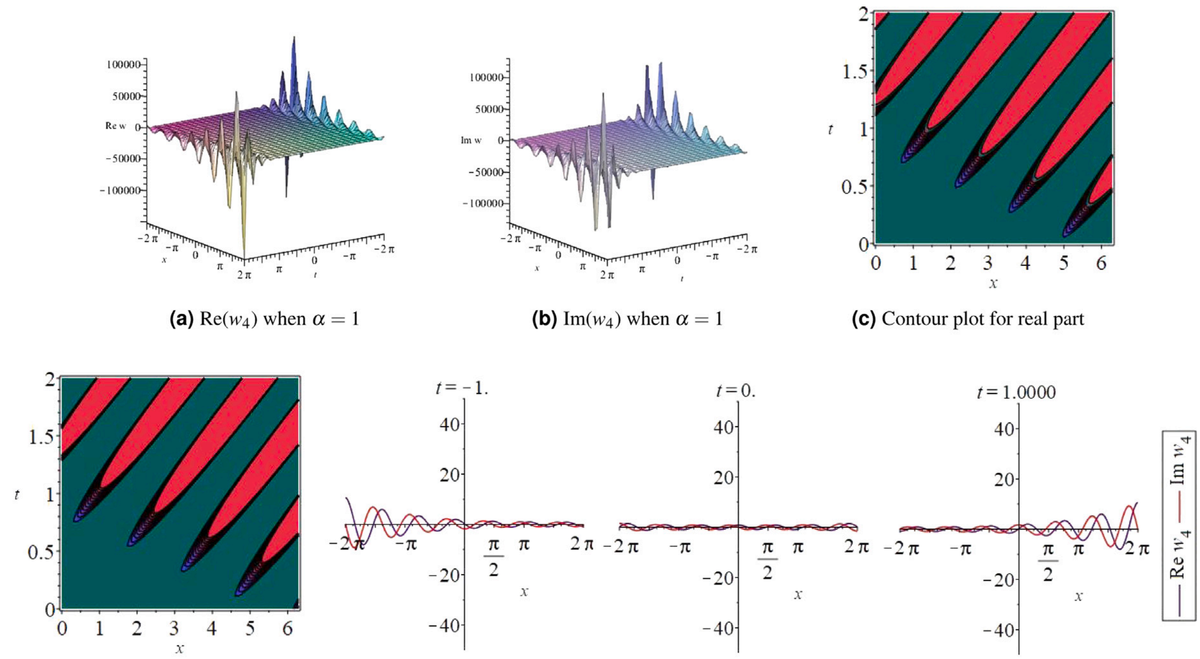

(a) Re(w_4) when $\alpha = 1$ (b) Im(w_4) when $\alpha = 1$ (c) Contour plot for real part

(d) Contour plot for imaginary part (e) 2D plot of the result w_4 at different times

Fig. 2. Outlook of (17) with the parametric values $k_1 = 0.2, m = 1, \alpha = 1, k = 0.3, c = 0, \epsilon = 0.1$.

(xvii) $P = \frac{m^2}{4}$, $Q = \frac{m^2-2}{2}$, $R = \frac{1}{4}, \xi = kx - v\frac{t^\alpha}{\alpha}$, $b = a^2 - a^3\epsilon - \epsilon\left(Q - 6\sqrt{PR}\right)k^3$.

$$w_{21}(x,t) = \left(\iota\sqrt{\frac{6}{4k_1+4k_2}}k\left(\frac{1 \mp dn(\xi)}{sn(\xi)}\right) + \iota\sqrt{\frac{6m^2}{4k_1+4k_2}}k\left(\frac{sn(\xi)}{1 \mp dn(\xi)}\right)\right) e^{\iota(ax-b\frac{t^\alpha}{\alpha}+c)}. \tag{34}$$

(xviii) $P = \frac{m^2-1}{4}$, $Q = \frac{m^2+1}{2}$, $R = \frac{m^2-1}{4}, \xi = kx - v\frac{t^\alpha}{\alpha}$, $b = a^2 - a^3\epsilon - \epsilon\left(Q - 6\sqrt{PR}\right)k^3$.

$$w_{22}(x,t) = \left(\iota\sqrt{\frac{6(m^2-1)}{4k_1+4k_2}}k\left(\frac{1 \mp msn(\xi)}{dn(\xi)}\right) + \iota\sqrt{\frac{6(m^2-1)}{4k_1+4k_2}}k\left(\frac{dn(\xi)}{1 \mp msn(\xi)}\right)\right) e^{\iota(ax-b\frac{t^\alpha}{\alpha}+c)}. \tag{35}$$

(xix) $P = -\frac{m^2-1}{4}$, $Q = \frac{m^2+1}{2}$, $R = \frac{m^2-1}{4}, \xi = kx - v\frac{t^\alpha}{\alpha}$, $b = a^2 - a^3\epsilon - \epsilon\left(Q - 6\sqrt{PR}\right)k^3$.

$$w_{23}(x,t) = \left(-\sqrt{\frac{6(m^2-1)}{4k_1+4k_2}}k\left(\frac{1 \mp sn(\xi)}{cn(\xi)}\right) + \iota\sqrt{\frac{6(m^2-1)}{4k_1+4k_2}}k\left(\frac{cn(\xi)}{1 \mp sn(\xi)}\right)\right) e^{\iota(ax-b\frac{t^\alpha}{\alpha}+c)}. \tag{36}$$

(xx) $P = \frac{(1-m^2)^2}{4}$, $Q = \frac{1+m^2}{2}$, $R = \frac{1}{4}, \xi = kx - v\frac{t^\alpha}{\alpha}$, $b = a^2 - a^3\epsilon - \epsilon\left(Q - 6\sqrt{PR}\right)k^3$.

$$w_{24}(x,t) = \left(\iota\sqrt{\frac{6}{4k_1+4k_2}}k\left(\frac{dn(\xi) \mp cn(\xi)}{sn(\xi)}\right) + \iota\sqrt{\frac{6(1-m^2)^2}{4k_1+4k_2}}k\left(\frac{sn(\xi)}{dn(\xi) \mp cn(\xi)}\right)\right) e^{\iota(ax-b\frac{t^\alpha}{\alpha}+c)}. \tag{37}$$

(xxi) $P = \frac{m^2}{4}$, $Q = \frac{m^2-2}{2}$, $R = \frac{1}{4}, \xi = kx - v\frac{t^\alpha}{\alpha}$, $b = a^2 - a^3\epsilon - \epsilon\left(Q - 6\sqrt{PR}\right)k^3$.

$$w_{25}(x,t) = \left(\iota\sqrt{\frac{6}{4k_1+4k_2}}k\left(\frac{\sqrt{1-m^2}sn \mp dn(\xi)}{cn(\xi)}\right) + \iota\sqrt{\frac{6(1-m^2)}{4k_1+4k_2}}k\left(\frac{cn(\xi)}{\sqrt{1-m^2} \mp dn(\xi)}\right)\right) e^{\iota(ax-b\frac{t^\alpha}{\alpha}+c)}. \tag{38}$$

Remark. The solitonic and trigonometric solutions can be acquired by taking limiting value of m which is shown in Table 2. A few such solutions are displayed here.

Dark soliton solution $\xi = kx - v\frac{t^\alpha}{\alpha}$, $b = a^2 - a^3\epsilon + 8\epsilon k^3$.

$$w(x,t) = \left(\iota\sqrt{\frac{6}{k_1+k_2}}k\left(\frac{1}{tanh(\xi)}\right) + \iota\sqrt{\frac{6}{k_1+k_2}}ktanh(\xi)\right)e^{\iota(ax-b\frac{t^\alpha}{\alpha}+c)}. \tag{39}$$

Singular dark soliton solution $\xi = kx - v\frac{t^\alpha}{\alpha}$, $b = a^2 - a^3\epsilon + 8\epsilon k^3$.

$$w(x,t) = \left(\iota\sqrt{\frac{6}{k_1+k_2}}k\left(\frac{1}{coth(\xi)}\right) + \iota\sqrt{\frac{6}{k_1+k_2}}kcoth(\xi)\right)e^{\iota(ax-b\frac{t^\alpha}{\alpha}+c)}. \tag{40}$$

Bright soliton solution $\xi = kx - v\frac{t^\alpha}{\alpha}$, $b = a^2 - a^3\epsilon - \epsilon k^3$.

$$w(x,t) = \left(-\sqrt{\frac{6}{k_1+k_2}}ksech(\xi)\right)e^{\iota(ax-b\frac{t^\alpha}{\alpha}+c)}. \tag{41}$$

Bright–Dark soliton solution $\xi = kx - v\frac{t^\alpha}{\alpha}$, $b = a^2 - a^3\epsilon - \epsilon k^3$.

$$w(x,t) = 2\iota\sqrt{\frac{6}{4k_1+4k_2}}k\left(\frac{sech(\xi)}{tanh(\xi)}\right)e^{\iota(ax-b\frac{t^\alpha}{\alpha}+c)}. \tag{42}$$

Singular soliton solution $\xi = kx - v\frac{t^\alpha}{\alpha}$, $b = a^2 - a^3\epsilon - \epsilon k^3$.

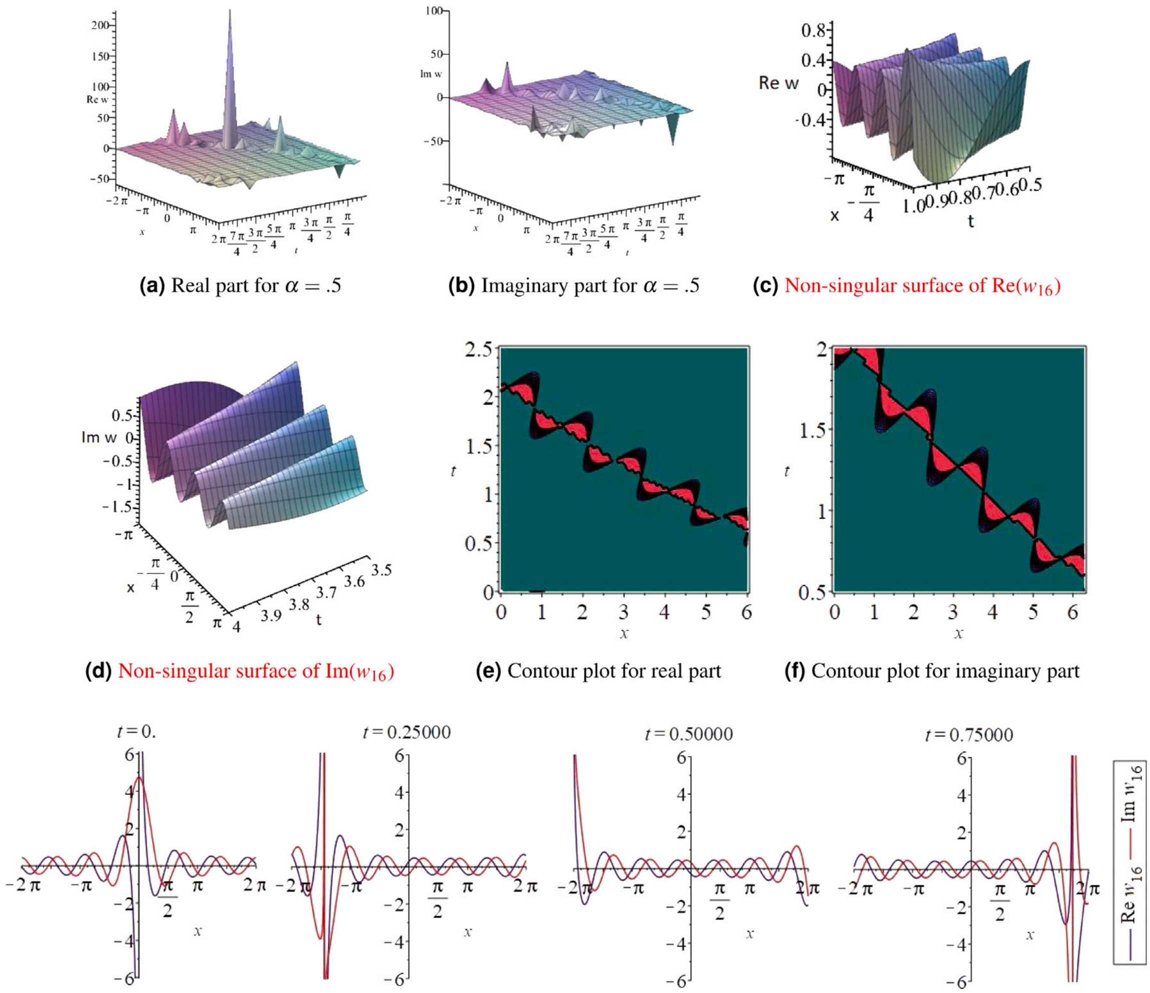

(a) Real part for $\alpha = .5$ **(b)** Imaginary part for $\alpha = .5$ **(c)** Non-singular surface of $\mathrm{Re}(w_{16})$

(d) Non-singular surface of $\mathrm{Im}(w_{16})$ **(e)** Contour plot for real part **(f)** Contour plot for imaginary part

(g) 2D profiles of the structure w_{16} at different times

Fig. 3. Plots of (29) with the parametric values $k_1 = 0.2, m = 0.8, \alpha = 0.5, k = 0.3, c = 0, \epsilon = 0.1$.

Table 2
Jacobi elliptic function for $m \to 0$ and $m \to 1$ [34,35].

	$m \to 0$	$m \to 1$		$m \to 0$	$m \to 1$		$m \to 0$	$m \to 1$
sn	*sin*	*tanh*	*dc*	*sec*	1	*sd*	*sin*	*sinh*
cn	*cos*	*sech*	*nc*	*sec*	*cosh*	*ds*	*csc*	*csch*
dn	1	*sech*	*sc*	*tan*	*sinh*	*nd*	1	*cosh*
cd	*cos*	1	*ns*	*csc*	*coth*	*cs*	*cot*	*csch*

$$w(x,t) = \left(\iota \sqrt{\frac{6}{k_1+k_2}}\, k\left(\frac{1}{csch(\xi)}\right) + \iota \sqrt{\frac{6}{k_1+k_2}}\, k\, csch(\xi)\right) e^{\iota(ax - b\frac{t^\alpha}{\alpha} + c)}. \tag{43}$$

Note 2: In all family of solutions, k_1, k, ϵ are free parameters while k_2, a, v are given in (10).

Numerical simulation

This section presents the graphical representations of some remarkable solutions of system (1), shown in the previous section, for specific values of parameters. The solutions exhibit periodical excitations as they come in terms of the combination of exponential and periodic sinusoidal functions. 3D graphical illustrations are given to show the spatio-temporal extension of the derived wave solutions, 2D projections, and their 2D contours are presented.

The 3D plots for real and imaginary parts of the solution $w_1(x,t)$ for the parametric values $k_1 = 0.2, m = 0.8, \alpha = 0.5, k = 0.3, c = 0, \epsilon = 0.1$ are shown in Fig. 1(a),1(b) respectively and their respective contours 1(e),1(f) show that the solution (14) exhibits periodic soliton solutions with multiple lumps of different peaks at which cusp type singularities exist. Also, the isolated singularities are featured at the points- $\cdots, -39.90605555, -26.60403704, -13.30201852, 0., 13.30201852, 26.60403704, 39.90605555, \ldots$ up to 8-digits accuracy when $t = 0$. The structures shown in 1(c) and 1(d) are non-singular for displacement $x = -\pi...\pi$ and evolution $t = 2...3$. The 1-dimensional wave propagation of real (indigo curve) and imaginary part (red curve) of the result (14) at time $t = 0, 0.21053, 0.42105, 0.63158$ are shown in 1(g) which show that a non-dispersive wave with group velocity greater than phase velocity moving in different directions. The wave group is formed by finite number of wave cycles oscillating between two consecutive discontinuities. To examine the dependence of the wave function on same parametric values, the surface plots 1(h),1(i) at $x = 1$ are shown for different values of α's. Increase in amplitude of wave function and accompanying phase shift with the increase of value of parameter α are evident in Fig. 1(h),1(i).

The 3D outlook for real and imaginary parts of solution (17) are given in 2(a),2(b) for $k_1 = 0.2, m = 1, \alpha = 1, k = 0.3, c = 0, \epsilon = 0.1$ and its contours are presented in 2(c),2(d) at spatial value $x = 1$. Clearly, w_{17} is non-singular everywhere. We observe that two parallel waves decay opposite. The wave motion represented for $t = -1, 0, 1$ in 2(e) depicts that wave group is a train of damped waves moving leftward.

We displayed the 2D wave propagation and 3D structures for real and imaginary parts of the solution $w_{16}(x,t)$ for the parametric values $k_1 = 0.2, m = 0.8, \alpha = 0.5, k = 0.3, c = 0, \epsilon = 0.1$ are in Fig. 3 respectively which shows the similar behavior as seen in Fig. 1. The isolated singularities are featured at the points- $\cdots, -26.60403704, -13.30201852, 0., 13.30201852, 26.60403704, \ldots$ up to 8-digits accuracy at initial time. We have drawn non-singular surfaces 3(c) and 3(d) for a certain displacement and time. The 1-dimensional wave propagation of real (indigo curve) and imaginary part (red curve) of the result w_{16} at time $t = 0, 0.25, 0.50, 0.75$ are shown in 3(g).

Conclusion

The authors obtained abundant wave solutions with rich physical structures of the complex nonlinear conformable time-fractional modified Schrödinger equation, which is having potential applications in the field of nonlinear optics, biological phenomena, and fluid dynamics, by using the GJEF method. Also, the Jacobi elliptic solutions can be used to obtain the solitary wave solutions, bright-dark optical solitons by limiting the modulus of Jacobi elliptic functions. In this kind of study, we can obtain the results for fractional as well as integer type PDEs in the same study. The obtained results show that this method is powerful and effective for constructing the periodic wave and optical soliton solutions of conformable fractional PDEs and the study may give a future scope in dealing with such kinds of equations. Also, the method is computable in software like Maple and Mathematica, which can ease tedious calculations.

CRediT authorship contribution statement

Pinki Kumari: Conceptualization, Software, Writing – original draft, Visualization. **R.K. Gupta:** Writing – review & editing, Investigation, Supervision. **Sachin Kumar:** Conceptualization, Writing – review & editing, Investigation, Supervision. **K.S. Nisar:** Software, Validation, Conceptualization.

Declaration of competing interest

The authors declare that they have no known competing financial interests or personal relationships that could have appeared to influence the work reported in this paper.

Acknowledgments

The author, Pinki Kumari, thanks to the University Grants Commission, India for the financial support via Ref. ID 19/06/2016(i)EU-V and the authors would like to extend their sincere appreciation to the Deanship of Scientific Research, King Saud University, Saudi Arabia for its funding through the Research Unit of Common First Year Deanship. The authors also acknowledge the anonymous reviewers for their valuable feedback and suggestions on an early draft of this article.

References

[1] Debnath L. Nonlinear partial differential equations for scientists and engineers. Springer Science & Business Media; 2011.
[2] Singh M. New exact solutions for (3+ 1)-dimensional Jimbo–Miwa equation. Nonlinear Dynam 2016;84:875–80.
[3] Singh M, Gupta R. Explicit exact solutions for variable coefficient Broer-Kaup equations. Comput Methods Differ Equ 2015;3:192–9.
[4] Singh M, Gupta R. Soliton and quasi-periodic wave solutions for b-type Kadomtsev–Petviashvili equation. Indian J Phys 2017;91:1345–54.
[5] Kumar S, Gupta R, Kumari P. A new pinlevé integrable Broer-Kaup system: symmetry analysis, analytic solutions and conservation laws. Internat J Numer Methods Heat Fluid Flow 2021.
[6] Kumari P, Gupta R, Kumar S. The time fractional d(m,n) system: invariant analysis, explicit solution, conservation laws and optical soliton. Waves Random Complex Media 2020;1–16.
[7] Kumari P, Gupta R, Kumar S. Non-auto-bäcklund transformation and novel abundant explicit exact solutions of the variable coefficients Burger equation. Chaos Solitons Fractals 2021;145:110775.
[8] Liu JG, Ye Q. Exact periodic cross-kink wave solutions for the (2+ 1)-dimensional Korteweg-de Vries equation. Anal Math Phys 2020;10:1–10.
[9] Liu JG, Du JQ, Zeng ZF, Nie B. New three-wave solutions for the (3+ 1)-dimensional Boiti–Leon–Manna–Pempinelli equation. Nonlinear Dynam 2017;88:655–61.
[10] Liu N, Guo B. Long-time asymptotics for the Sasa–Satsuma equation via nonlinear steepest descent method. J Math Phys 2019;60:011504.
[11] Liu JG, Zhu WH, Osman M, Ma WX. An explicit plethora of different classes of interactive lump solutions for an extension form of 3D-Jimbo–Miwa model. Eur Phys J Plus 2020;135:412.
[12] Liu JG, Xiong WP. Multi-wave,breather wave and lump solutions of the Boiti–Leon–Manna–Pempinelli equation with variable coefficients. Results Phys 2020;19:103532.
[13] Liu JG, Zhu WH. Multiple rogue wave, breather wave and interaction solutions of a generalized (3+ 1)-dimensional variable-coefficient nonlinear wave equation. Nonlinear Dynam 2021;103:1841–50.
[14] Liu JG, Osman M. Nonlinear dynamics for different nonautonomous wave structures solutions of a 3D variable-coefficient generalized shallow water wave equation. Chinese J Phys 2021.
[15] Liu J-G, Zhu W-H, He Y. Variable-coefficient symbolic computation approach for finding multiple rogue wave solutions of nonlinear system with variable coefficients. Z. FÜr Angew. Math Und Phys 2021;72:1–12.
[16] Tian Y, Liu J-G. Study on dynamical behavior of multiple lump solutions and interaction between solitons and lump wave. Nonlinear Dynam 2021;104:1507–17.
[17] San S, Kumari P, Kumar S. On analytic series solutions and conserved fluxes of the time fractional (2+1)-dimensional burger's system via invariant approach. Waves Random Complex Media 2021;1–13, https://doi.org/10.1080/17455030.2021.2005848.
[18] Raza N. Exact periodic and explicit solutions of the conformable time fractional Ginzburg Landau equation. Opt Quantum Electron 2018;50:154.
[19] Korkmaz A, Hosseini K. Exact solutions of a nonlinear conformable time-fractional parabolic equation with exponential nonlinearity using reliable methods. Opt Quantum Electron 2017;49:278.
[20] Shallal MA, Ali KK, Raslan KR, Rezazadeh H, Bekir A. Exact solutions of the conformable fractional EW and MEW equations by a new generalized expansion method. J Ocean Eng Sci 2020.
[21] Yaslan HÇ. New analytic solutions of the conformable space–time fractional kawahara equation. Optik 2017;140:123–6.
[22] Das A. Optical solitons for the resonant nonlinear schrödinger equation with competing weakly nonlocal nonlinearity and fractional temporal evolution. Nonlinear Dynam 2017;90:2231–7.
[23] Kumari P, Gupta R, Kumar S, Al Qurashi MM. Erratum to "conserved vectors with conformable derivative for certain systems of partial differential equations with physical applications". Open Phys 2020;18:1108–10.
[24] Kodama Y. Optical solitons in a monomode fiber. J Stat Phys 1985;39:597–614.
[25] Potasek M, Tabor M. Exact solutions for an extended nonlinear Schrödinger equation. Phys Lett A 1991;154:449–52.
[26] Abdeljawad T. On conformable fractional calculus. J Comput Appl Math 2015;279:57–66.
[27] Rezazadeh H others. New optical solitons of nonlinear conformable fractional Schrödinger-Hirota equation. Optik 2018;172:545–53.
[28] Benia Y, Ruggieri M, Scapellato A. Exact solutions for a modified Schrödinger equation. Mathematics 2019;7:908.
[29] Daniel M, Latha M. A generalized davydov soliton model for energy transfer in alpha helical proteins. Physica A 2001;298:351–70.
[30] Khalil R, Al Horani M, Yousef A, Sababheh M. A new definition of fractional derivative. J Comput Appl Math 2014;264:65–70.
[31] Zhao D, Luo M. General conformable fractional derivative and its physical interpretation. Calcolo 2017;54:903–17.
[32] Huai-Tang C, Hong-Qing Z. New double periodic and multiple soliton solutions of the generalized (2+1)-dimensional Boussinesq equation. Chaos Solitons Fractals 2004;20:765–9.
[33] Uğrlu Y, Kaya D, Inan IE. Generalized Jacobi elliptic function method for periodic wave solutions of SRLW equation and (1+1)-dimensional dispersive long wave equation. ÇAnkaya üniversitesi Bilim Ve Mühendislik Dergisi 2011;8.
[34] Hua-Mei L. New exact solutions of nonlinear Gross–Pitaevskii equation with weak bias magnetic and time-dependent laser fields. Chin Phys 2005;14:251.
[35] Tasbozan O, Kurt A, Tozar A. New optical solutions of complex Ginzburg–Landau equation arising in semiconductor lasers. Appl Phys B 2019;125:104.